# Theoretical Study of Reaction Pathways of Dibenzofuran and Dibenzo-*p*-Dioxin under Reducing Conditions

**Mohammednoor Altarawneh, Bogdan Z. Dlugogorski,* Eric M. Kennedy, and John C. Mackie***

*Process Safety and Environment Protection Research Group, School of Engineering, The University of Newcastle, Callaghan, NSW 2308, Australia*

*Received: February 11, 2007; In Final Form: May 2, 2007*

A density functional theory (DFT) study was carried out to investigate possible reactions of dibenzofuran (DF) and dibenzo-*p*-dioxin (DD) in a reducing environment. Reaction energies, barrier heights, and molecular parameters for reactants, intermediates, products, and transition states have been generated for a wide range of possible reactions. It was found that C−O $\beta$-scission in DF incurs a very large energy barrier (107 kcal/mol at 0 K), which is just 3 kcal/mol less than the direct H fission from C−H in DF to form dibenzofuranyl radicals. It was found that DF allows direct H addition to C1−C4 and C6−C9 as well as addition of two H atoms from a hydrogen molecule at sites 1 and 9 of DF. A bimolecular reaction of DF with H or $H_2$ is found to have a significantly lower barrier than unimolecular decomposition through C−O $\beta$-scission. An explanation for the predominance of polychlorinated dibenzofurans (PCDF) over polychlorinated dibenzo-*p*-dioxins (PCDD) in municipal waste pyrolysis is presented in the view of the facile conversion of DD into DF through ipso-addition at the four C sites of the two C−O−C central bonds in DD.

## 1. Introduction

Polychlorinated dibenzo-*p*-dioxins and dibenzofurans (PCDD/F) have been studied extensively, owing to their highly toxicological effects.[1] Many of these studies have been oriented to gain a better understanding of the formation and decomposition pathways of PCDD/F. PCDD/F are formed as byproducts in industrial and combustion systems when chlorine is present,[2] including the thermal treatment of municipal waste. Pyrolysis treatment of municipal waste is being developed on an industrial[3,4] scale as an alternative to the existing incineration systems. Operating conditions in terms of temperature profile, oxygen content, and residence time are different in pyrolysis from those present in combustion, especially since pyrolysis of municipal waste is conducted at temperatures from 450 to 700 °C,[4] the range which spans the upper window of PCDD/F formation.

The ratio of PCDD to PCDF in pyrolysis of municipal waste differs significantly from that observed in municipal waste incineration (MWI);[5,6] up to 400 times more PCDF are produced in pyrolysis compared to PCDD,[4] while the ratio of PCDD to PCDF in a typical incinerator ranges from 0.4 to 10.[7] Moreover, the degree of chlorination is shifted considerably toward the lower chlorinated congeners as a consequence of low oxygen content in pyrolysis (0.5−2%). Mechanisms of PCDD/F formation during pyrolysis are not fundamentally different from those that take place during incineration, based on finding similar isomer patterns of PCDD/F in the two systems.[4] Formation of PCDD/F from 2-chlorophenol precursors under oxidative and reducing conditions has been investigated both experimentally[8,9] and theoretically.[10] While the shift toward lower chlorinated congeners follows from the suppression of the Deacon reaction cycle and oxychlorination from metal chlorides, the high yield of PCDF compared with PCDD in pyrolysis deserves further explanation.

In pyrolysis, competition exists between the self-decomposition of reactants and primary products and their reactions with H atoms and $H_2$. Pyrolysis of PCDD/F has been studied experimentally for the nonchlorinated dibenzo-*p*-dioxin (DD) by Cieplik et al.[11] and nonchlorinated dibenzofuran (DF) by Cieplik et al.[11] and Winkler et al.[12] In the study of Cieplik et al., pyrolysis was conducted in an excess of hydrogen (thermal hydrogenolysis). Since DD and DF rings constitute the major functional parts of PCDD/F, these two studies present valuable information on the behavior of PCDD/F under pyrolytic conditions. Both DD and DF produce CO and ethane as major decomposition species in addition to trace amounts of naphthalene and benzene. Interestingly, DF is an important product in DD pyrolysis with a selectivity of 50%. It has been reported[11] that the rate of disappearance of DD strongly depends on the concentration of hydrogen atoms while DF consumption is insensitive to the concentration of $H_2$. Cieplik et al.[11] have found that DF under conditions of excess $H_2$ reacts 4000 times slower than DD. Thus, these researchers concluded that DF consumption proceeds via C−O $\beta$-scission, rather than through a reaction with either hydrogen molecule or hydrogen atom.

In our previous study, a detailed mechanism derived by density functional theory (DFT)[13] was presented for DF decomposition through reactions with molecular oxygen. This mechanism was found to be in accordance with the experimental results. In the present study, DFT is employed to determine the energetics of the self-decomposition of DF, and the reactions of DF and DD with $H_2$ and H. The results enable us to comment qualitatively on the experimental results presented previously.[4,11,12]

DFT has been utilized in earlier studies investigating the behavior of PCDD under reducing conditions.[14,15] In these

* Corresponding author. E-mail: Bogdan.Dlugogorski@newcastle.edu.au, Fax: (+61 2) 4921 6920; Tel: (+61 2) 4921 6176.

10.1021/jp071166q CCC: $37.00 
Published on Web 07/04/2007

**TABLE 1: Barrier Heights (kcal/mol) for Hydrogen Addition Reactions Calculated by B3LYP and BB1K Methods**

| reaction | B3LYP/6-311+G(3df,2p)// B3LYP/6-31G(d) | BB1K/6-311+G(3df,2p)// BB1K/6-31G(d) |
|---|---|---|
| DF + H → VI | 2.9 | 4.4 |
| DF + H → IX | 6.5 | 9.0 |
| DF + H → XI | 7.8 | 10.4 |
| DF + H → XIII | 36.5 | 46.8 |
| DF + H2 → IV | 70.1 | 78.3 |
| DF + H2 → V | 91.4 | 98.6 |
| DD + H → XVI | 5.3 | 7.6 |
| DD + H → XIV | 31.6 | 37.5 |

studies, dechlorination of PCDD by hydrogen atoms has been elucidated as a mechanism responsible for lowering the overall toxicity of PCDD/F. Herein, theoretical investigations are carried out to study other important reaction pathways besides dechlorination that PCDD/F are most likely to encounter in a highly reducing environment such as that existing in the pyrolysis of municipal waste. Comparison is also made with available experimental results on the reactivity of DD and DF under reducing conditions.

## 2. Computational Methods

Throughout this study, B3LYP incorporated in the *Gaussian 03*[16] code was used to obtain optimized geometries and harmonic vibrational frequencies of all reactants, products, and transition structures on the reaction energy hypersurfaces. B3LYP employs the three-parameter Becke exchange functional, B3,[17] with the Lee−Yang−Parr nonlocal correctional functional LYP[18] with the polarized basis set of 6-31G(d).[19] Concerning B3LYP performance on dioxin-like compounds, the adopted computational approach of B3LYP in this study (i.e., basis set, single point energy calculations) has been used by Zhu and Bozzelli[20] to calculate heats of formation ($\Delta_f H^\circ_{298}$) for PCDD/F compounds.

The calculated values for $\Delta_f H^\circ_{298}$ of dibenzo-*p*-dioxin (DD) and dibenzofuran (DF) are −51.8 kJ/mol and 58.2 kJ/mol,[20] respectively, compared with experimental values of −50.1 ± 2.2 kJ/mol[21] and 55.3 ± 0.35 kJ/mol,[22] respectively. The difference between experimental and calculated values of $\Delta_f H^\circ_{298}$ obtained in that study can be taken as an estimation of the expected error margins in our B3LYP calculations for energies of stable molecules. In terms of geometries, the B3LYP method yields very good agreement when compared with structural parameters and vibrational frequencies obtained experimentally. Detailed comparisons between calculated and experimental values have been presented by Okamoto et al.[23] Thus, on the basis of the available literature data, we expect the accuracy of our calculations using the B3LYP method to be acceptably high for reaction energies, vibrational frequencies, and structural parameters.

As we are aware of the fundamental shortcoming of the B3LYP method in determining the shape of the potential energy surface (PES) around the transition structure position of H addition reactions due to its inadequate description of the self-interaction correction,[24−26] barrier heights for H and $H_2$ addition reactions were also computed by the BB1K method (Table 1).[27] The BB1K method is one of the meta hybrid DFT methods such that, in addition to using an HF exchange fraction, it also abstracts kinetic energy density from Kohn−Sham orbitals. The successful approach of BB1K in determining barrier heights was obtained using an HF exchange fraction of 0.42 (compared with 0.20 in B3LYP), but also in deploying the kinetic-energy-dependent dynamical correlation functional BB95.[28] BB1K has been shown to significantly outperform all hybrid DFT methods including B3LYP in saddle-point geometries and barrier heights, especially for hydrogen transfer reactions.[29] However, B3LYP was shown to be slightly more effective in obtaining bond energies and stable molecular structures. It is worth pointing out that performing single-point energy calculations with coupled cluster including single excitation (CCS) has been used as a successful approach to cure the shortcomings of B3LYP in predicting energy barriers for hydrogen addition reactions.[30] However, such calculations are not feasible for the system at hand due to its high computational requirements.

As we are concerned with relatively large molecular species, high-accuracy methods such as G3 are not appropriate; thus, single-point energy calculations with the extended basis set of 6-311+G(3df,2p) have been performed on the geometry obtained with the 6-31G(d) basis set to obtain reliable energies. Stationary points (energy minima, transition states) were classified through diagonalization of the analytical Hessian (number of imaginary frequency NIMAG = 0 for energy minima and 1 for transition states).

For certain structures that might express a singlet biradical structures, such as transition states for hydrogen molecule addition to DF and for C−O $\beta$-bond scission, the ground-state wave function was tested as to whether it is open- or closed-shell by first calculating the triplet electronic state of these structures on the basis of geometries optimized previously by the B3LYP method. Reoptimization using the unrestricted UB3LYP through reading orbitals generated from the triplet state as an initial guess for the wavefunction yields structures with the same geometries and energies and a zero value for the $\langle S^2 \rangle$ operator as were obtained using the restricted RB3LYP method. Thus, the ground-state wavefunctions for these structures are closed-shell. Where appropriate, intrinsic reaction coordinate (IRC) calculations have been used to link the reactant and product with their transition structures.

The most important interatomic features of the transition states are displayed in the figures. For several reactions in the self-decomposition of DF and its reaction with $H/H_2$, rate constants have been calculated using conventional transitional-state theory.[31]

## 3. Results and Discussion

**3.1. DF System.** The presently accepted mechanistic pathways for the decomposition of DF under reducing conditions, in the presence of hydrogen, are those of Cieplik et al.[11] These investigators have argued that unimolecular $\beta$-bond scission of the C−O bridge initiates DF decomposition, based on the observed lack of dependence of the DF decomposition rate on the concentration of molecular hydrogen. Here, we present theoretical calculations of the various channels associated with unimolecular DF decomposition and bimolecular reactions with H and $H_2$, to determine the veracity of the existing mechanism for the decomposition of DF.

*3.1.1. Unimolecular Decomposition of DF.* Unimolecular decomposition of DF could be initiated either by C−H or C−O bond scission, because both these bonds are significantly weaker than the aromatic C−C bond. The calculated C−H bond energies in DF range from 110 to 112 kcal/mol (at 0 K); H fission occurs without an intrinsic barrier. Dimers and trimers of DF were observed in the mass spectrometer,[12] indicating that dibenzofuranyl radicals are formed through H fission despite the high endothermicity of this reaction. In the experimental study of Cieplik et al.,[11] the most direct unimolecular channel was assumed to proceed via O−C bond scission. The calculated energy of O−C bond scission using RB3LYP is 98.2 kcal/mol

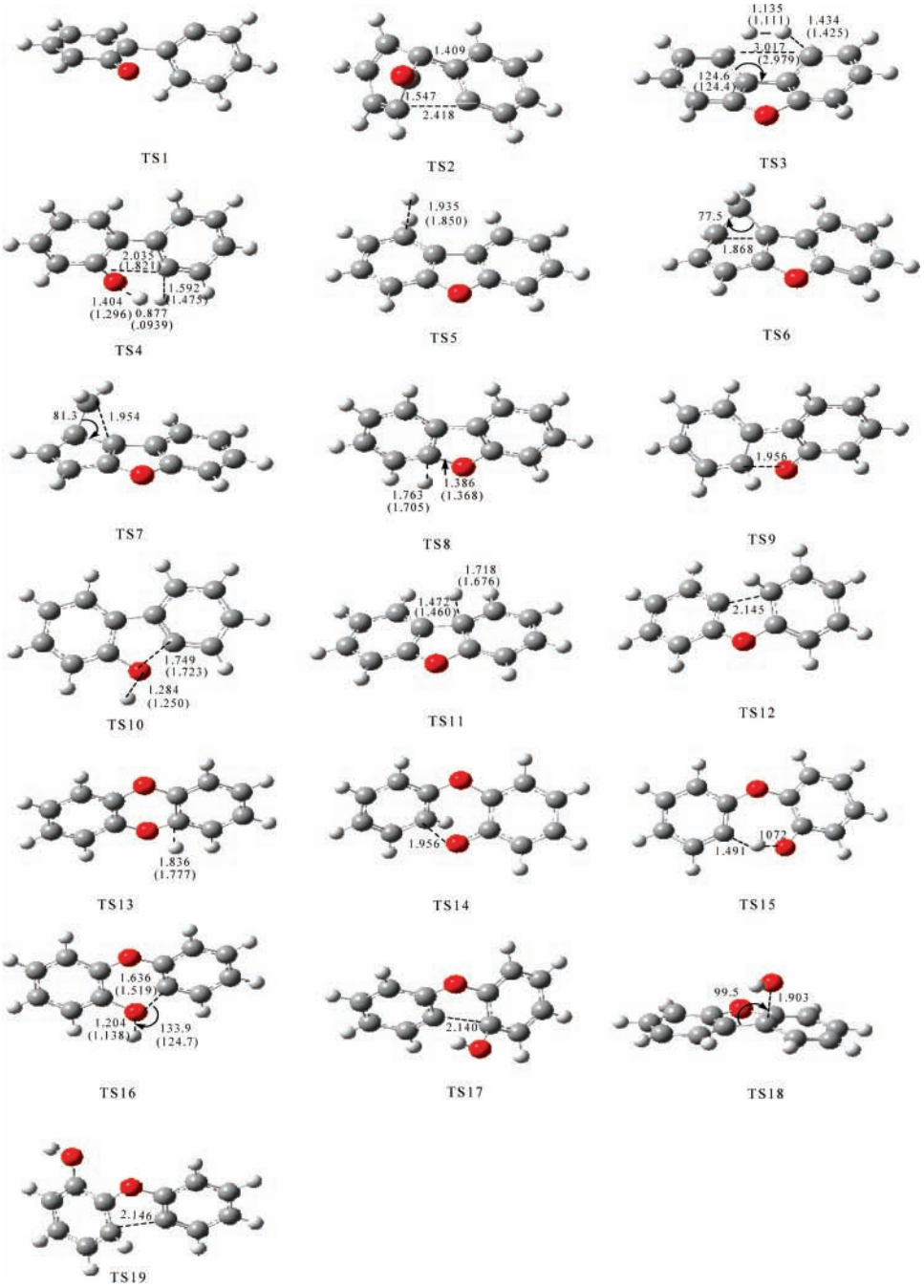


**Figure 1.** Optimized geometries (bond lengths in angstroms and angles in degrees) of transition structures at the B3LYP/6-31G(d) level of theory. Values are shown in brackets for transition structures of hydrogen addition reactions calculated by BB1K/6-31G(d) level of theory.

(0 K) with a barrier height of 107.1 kcal/mol passing through TS1, as illustrated in Figure 1. In the optimized structure (I in Figure 2), the C and O atoms are rotated by 180°, while this rotation is 90° in the transition state. Note that no equilibrium structures could be obtained where both C and O were in the same plane or even rotated to a degree other than 90° (TS1) or 180° (I).

Although the energy requirements of the two processes are very similar, the H loss channel is expected to be more important than the C−O bond scission due to entropic effects associated with species generation in the unimolecular reaction. Entropies and enthalpies calculated by conventional transition-state theory have been used to obtain the nonlinear Arrhenius pre-exponential factor ($AT^n$) and energy of activation to yield the high-pressure rate constant, $k_\infty(T)$, for reaction 1 as a function of temperature, given in Table 2. The observed unimolecular rate constant of disappearance of DF was found to be $\log k/s^{-1} = 13.3 - (76.6 \text{ kcal/mol})/2.3RT$.[11] At temperatures between 1133 and 1213 K, the observed rate constant for DF disappearance is faster than that calculated for reaction 1 by more than 4 orders of magnitude. Thus, our quantum chemical calculation does not support a DF self-decomposition channel through C−O $\beta$-bond scission.

To investigate more fully the self-decomposition pathway, the potential energy surface (PES) has been plotted in Figure 3 for the subsequent reaction steps after the bond fission as proposed in Cieplik et al.[11] The product flux to naphthalene was supposed to pass through the reactions I → II (5*H*-5,9-methanobenzo[7]annulen-10-one, structure II in Figure 2) → III (5*H*-benzo[7]annulen-5-ylidenemethanone, structure III in Figure 2). However, as indicated in Figure 3, this pathway is highly unlikely due to the very high energy barrier (147.6 kcal/

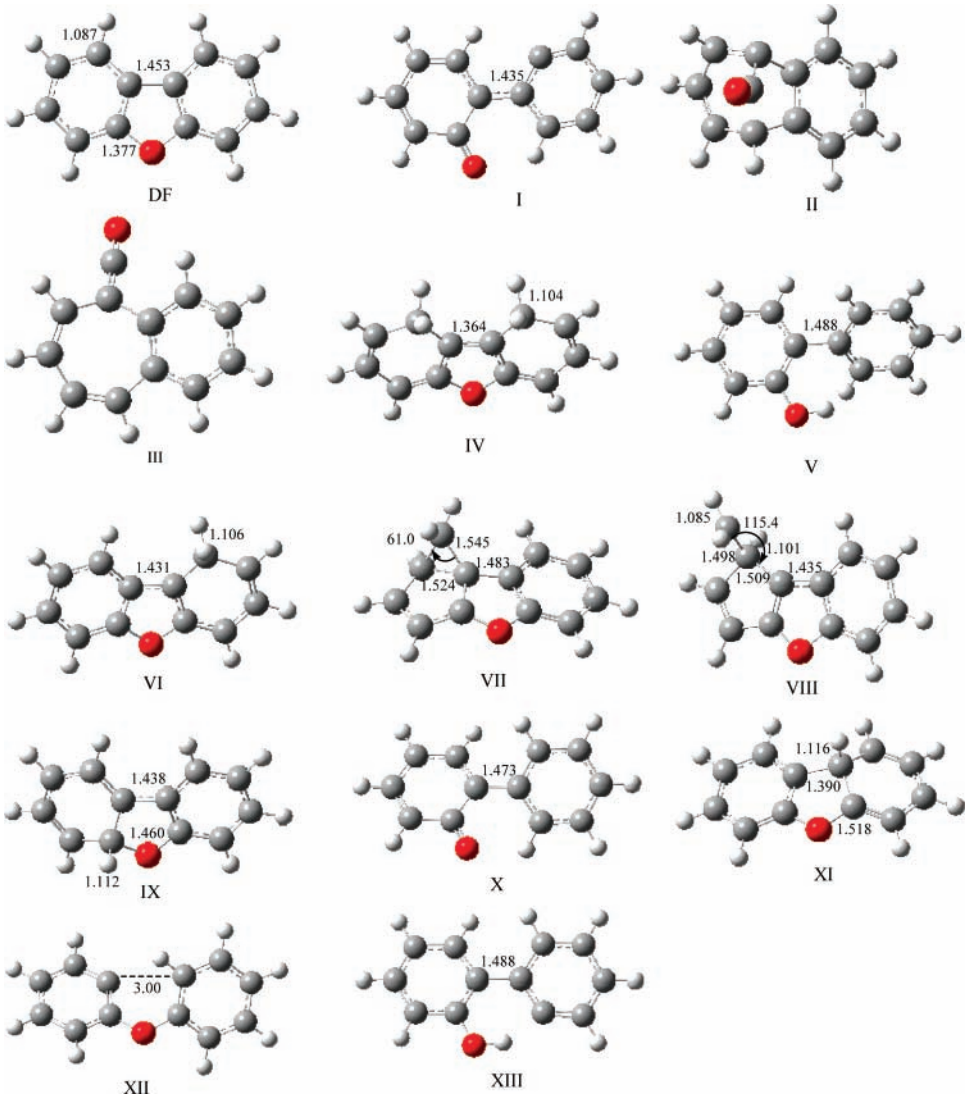


**Figure 2.** Optimized geometries (bond lengths in angstroms and angles in degrees) of reactant and intermediates at the B3LYP/6-31G(d) level of theory.

**TABLE 2: Calculated Rate Constants for Key Reactions**[a]

| no. | reaction | TS | $A$ | $n$ | $E_a$ (kcal/mol) | units |
|---|---|---|---|---|---|---|
| 1 | DF → I | TS1 | $1.7 \times 10^{12}$ | 0.76 | 108.4 | $s^{-1}$ |
| 2 | DF + H2 → IV | TS3 | $1.8 \times 10^{12}$ | 0.0 | 74.9 | $cm^3\ mol^{-1}\ s^{-1}$ |
| 3 | DF + H2 → V | TS4 | $7.8 \times 10^{13}$ | 0.0 | 96.7 | $cm^3\ mol^{-1}\ s^{-1}$ |
| 4 | DF + H → IX | TS8 | $6.2 \times 10^{13}$ | 0.0 | 8.5 | $cm^3\ mol^{-1}\ s^{-1}$ |
| 5 | DF + H → XI | TS9 | $5.8 \times 10^{13}$ | 0.0 | 10.2 | $cm^3\ mol^{-1}\ s^{-1}$ |

[a] B3LYP was used to calculate the rate constant for reaction 1 and BB1K for reactions 2−5.

mol at 0 K) relative to DF. Thus, the two unimolecular channels for DF decomposition, especially C−O bond scission, could not account for products yield from DF pyrolysis and are expected to be slow when compared with bimolecular reaction of DF with $H_2$ and/or H in the pyrolytic environment. A detailed description of pathways and energetics of these reactions is given in the next section.

*3.1.2. Bimolecular Reactions of DF with $H_2$ and H.* All barriers for hydrogen addition reactions calculated by B3LYP and BB1K are reported in Table 1. In all cases, barrier heights are lower for the B3LYP method. These results are consistent with the general feature of B3LYP underestimating the energy barriers. According to the PES shown in Figure 4, two channels for the $H_2$ + DF reaction are feasible. The first is characterized by addition of both H atoms from the hydrogen molecule at sites 1 and 9 of DF to form adduct IV. The TS3 of this reaction was optimized using B3LYP and BB1K methods. In accord with the reaction endothermicity, TS3 has a product-like character. In the optimized structure obtained by the B3LYP method, the H−H bond length is 1.135 Å, about 55% longer than the equilibrium bond length in $H_2$, and the new C−H bond is 1.434 Å. The hydrogen molecule additions are endothermic by 35.3 kcal/mol (0 K) with a computed barrier height of 70.1 kcal/mol by the B3LYP method; this barrier increases to 75.4 kcal/mol when optimized with the BB1K method. Thus, reaction between DF + $H_2$ is energetically favored over C−O bond fission. H addition makes the C−C bridge shorter by 0.089 Å. The C−H bond in DF is displaced from the molecular plane by 7°, a displacement which has also been observed for addition of two H atoms to benzene.[32] C−H bonds at sites 1 and 9 are elongated by 0.017 Å, enabling H eliminations from the two hydrogenated sites to take place with endothermicity of ap-

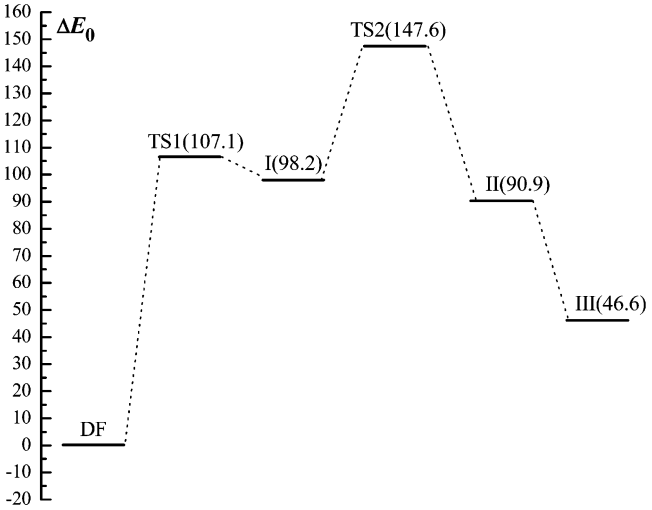


**Figure 3.** Schematic pathway for unimolecular pyrolysis of dibenzofuran (DF) induced by the fission of C−O bond. Reaction energies with ZPE corrections (in kcal/mol) are calculated at the B3LYP/6-311+G(3df,2p)//B3LYP/6-31G(d) level of theory.

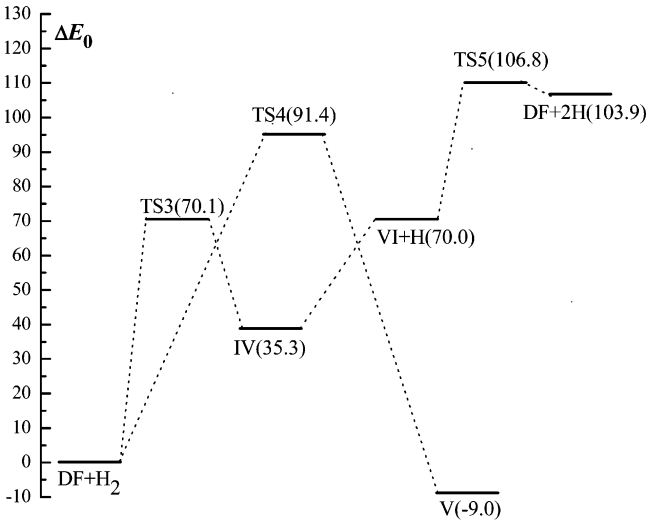


**Figure 4.** Schematic pathways for the reaction DF + $H_2$. Reaction energies with ZPE corrections (in kcal/mol) are calculated at the B3LYP/6-311+G(3df,2p)//B3LYP/6-31G(d) level of theory. (More accurate barriers for hydrogen addition reactions calculated by BB1K method are reported in Table 1.)

proximately 35 kcal/mol (reactions IV → VI + H and VI → TS5 → DF + H). This is significantly lower than the value of about 110 kcal/mol required for H elimination from DF itself.

The second reaction channel for reactants $H_2$ and DF is slightly exothermic, producing 2-hydroxybiphenyl (structure V in Figure 2) via a barrier of 98.6 kcal/mol (TS4) using the BB1K method. This bimolecular channel has been suggested by Winkler et al.[12] from their experimental studies of pyrolysis of DF in argon in which it is supposed that $H_2$ forms subsequently after H fission from DF in forming dibenzofuranyl radicals.

H atom reaction with DF proceeds through several channels as shown in the doublet hypersurfaces displayed in Figure 5. The first channel involves direct H addition to the oxygen in the center of the C−O−C bridge in DF to produce structure XIII in a slightly exoergic reaction of −1.5 kcal/mol (0 K). The reactants climb a sizable barrier of 36.5 kcal/mol characterized by the transition structure TS10 in Figure 1 calculated by B3LYP/6-31G(d) (with single-point calculation with the larger 6-311+G(3df,2p) basis set). This barrier becomes significantly higher by 10.3 kcal/mol when calculated by the BB1K method. The second reaction channel is actually the reverse of the reaction in which H is expelled from VI. (Other analogous reactions at positions 2−4 are also to be expected.) The addition of a single H atom to DF via this channel stabilizes VI by 26.7 kcal/mol (0 K). In TS5, despite the hydrogen atom being distant by 1.935 Å from the DF moiety, it nevertheless has the effect of elongating the neighboring C−C bonds by 0.012 Å. The formation of VIII, with the $CH_2$ group out-of-plane, requires an activation energy of 45.3 kcal/mol to take place through TS6. Structure VIII can be regarded as a direct precursor for the observed cyclopentadiene derivatives[11] with overall endoergicity of 12 kcal/mol and overall barrier of 24.5 kcal/mol (0 K).

Other channels proceed through ipso-addition to the central C−C and C−O bonds. H atom addition at the carbon atom of the C−O bond requires only 9.0 kcal/mol of activation energy using the BB1K method, while it is less energy-demanding by 2.5 kcal/mol using the B3LYP method. The reaction is exoergic by 15.4 kcal/mol. This produces the adduct IX. Ipso-addition of H at this site enables facile rupture of the C−O bond in structure IX, leading to the formation of structure X with 16.1 kcal/mol of exothermicty. Using the BB1K method, H addition to the C−C bridge has a barrier of 10.4 kcal/mol and passes through the loose transition state TS11; this channel proceeds until the C−C bond breaks, producing structure XII with an overall endoergicity of 6.2 kcal/mol and overall energy barrier of 16.4 kcal/mol (TS12). The reverse barriers for both ipso-addition reactions are found to be greater than the forward barriers. The opposite argument had been advanced previously[11] to explain that there would be no effective ipso-addition at the two sites considered, because it had been assumed that the reverse reactions would dominate.

Consider now a comparison between the calculated rate constants for $H_2$ reaction with DF and the experimental rate for DF disappearance under thermal hydrogenolysis conditions. The limiting high-pressure rate constants for reaction between DF and $H_2$ to give IV, V, IX, and XI, respectively, are reported in Table 2 (reactions 2−5). With the experimental conditions of ref 11, viz., 35 bar of molecular hydrogen and a temperature of 1173 K, the observed first-order reaction rate constant for DF disappearance is 0.098 $s^{-1}$, and the pseudo-first-order rate constant (i.e., $k_2[H_2]$) obtained from the calculated bimolecular rate constant (reaction 2 in Table 2) for 35 bar of $H_2$ is only $0.068 \times 10^{-2}$ $s^{-1}$. Thus, the experimental rate constant for DF disappearance is 140 times faster than the theoretical pseudo-first-order rate constant for two H additions to DF in excess hydrogen. However, subsequent bimolecular reactions between H atoms (e.g., from fission of H from structure IV as shown in the PES of Figure 4) and DF would greatly accelerate the rate of disappearance of DF and can lead to modeled rates of disappearance of DF similar to those observed experimentally.

Although our DFT calculations of the initial rate for DF disappearance (based solely on molecular reaction between DF and $H_2$) are not in quantitative agreement with experimental findings,[11] our calculations do establish the following:

(i) It is clear that the rate of DF consumption in pyrolysis, especially in the presence of excess hydrogen (thermal hydrogenolysis), does not involve the initial C−O bond fission, since this requires an energy barrier even higher than direct H scission from a C−H bond of DF.

(ii) DF does react with $H_2$, in contrast with the interpretation of the experimental results of ref 8 and in accordance with the experimental findings of Winkler et al.[12]

(iii) Ipso-addition of H atom to the central C−C and C−O bonds readily produces DF fragmentation rather than equilibra-

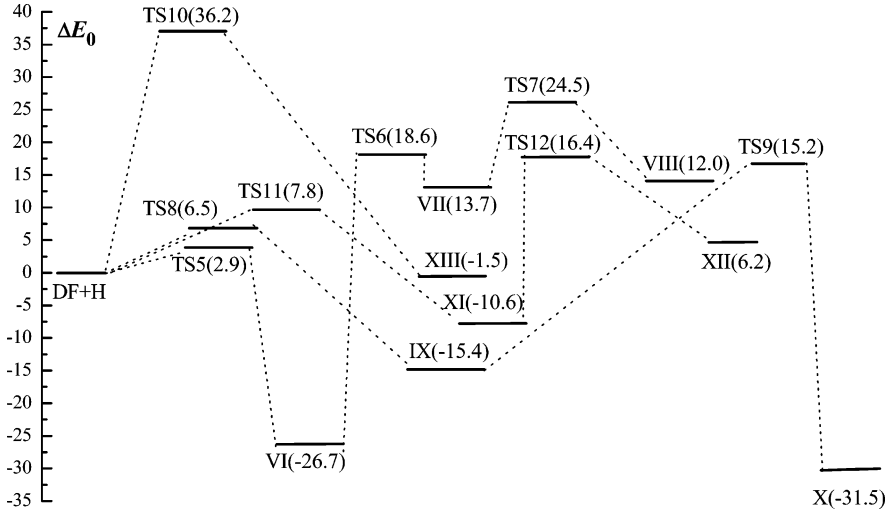


**Figure 5.** Schematic pathways for the reaction DF + H. Reaction energies with ZPE (in kcal/mol) are calculated at the B3LYP/6-311+G(3df,-2p)//B3LYP/6-31G(d) level of theory. (More accurate barriers for hydrogen addition reactions calculated by BB1K method are reported in Table 1.)

tion via the reverse reaction to H and DF, as suggested previously.[11]

The discrepancy between experimental and theoretical predictions for the rate of disappearance of DF can also be attributed to the formation of H atoms from $H_2$ arising from an external source such as a catalytic wall effect. Combining the unimolecular rate constant for DF disappearance through C−O bond scission and bimolecular reactions of DF with H and $H_2$ is expected to bring the theoretical predictions closer to the experimental rate constant for DF disappearance. Concerning the apparent insensitivity of DF toward reaction with molecular hydrogen, the two theoretically available channels require very high energy barriers (78.3 and 98.6 kcal/mol); thus, these two reactions would be slow at the temperature region over which the experiment was conducted (1157−1262 K), resulting in the observed insensitivity to variation of the hydrogen molecule concentration.

**3.2. DD System: Bimolecular Reactions of DD with H and Conversion of DD into DF.** The reaction of H with PCDD has previously been studied by ab initio calculations for 1,2,3,4,6,7,8,9-octachlorodibenzo-*p*-dioxin (OCDD)[14] and for 2,3,7,8-tetrachlorodibenzo-*p*-dioxin for (2,3,7,8-TCDD).[15] Fueno et al.[14] have assessed the regioselectivity of the OCDD and H system to determine whether chlorine atom abstraction by H from OCDD would lead predominantly to the most toxic congener, viz., 2,3,7,8-TCDD. H either abstracts Cl directly to form HCl or acts through ipso-addition followed by Cl elimination. At the density functional B3PW91/3-21G** level of theory, Fueno et al.[14] found that the barrier for direct Cl abstraction by H to form HCl is 8.8 kcal/mol, whereas H addition and subsequent Cl elimination required a barrier of about 5.3 kcal/mol.

Okamoto[15] proposed a scheme for decomposition of TCDD involving H irradiation. This required two steps, a successive abstraction of chlorine by H induced by hydrogen irradiation, followed by C−O bond fission. In this process, a dative bond formed between the O atom of the broken C−O bond and H stabilizes the system, while a hydrogen radical attaches to the C site. This makes the C−O bond elongate significantly until a chemical bond can be formed between O and H. Okamoto[15] assumed that the chlorine abstraction is rate-determining for that decomposition pathway.

Herein, we investigate C−O bond fission of DD (the weakest among the seven distinguishable bonds that form DD) in order to simulate typical reducing conditions in municipal waste pyrolysis so as to establish whether Cl elimination or C−O bond fission dominates the decomposition process.

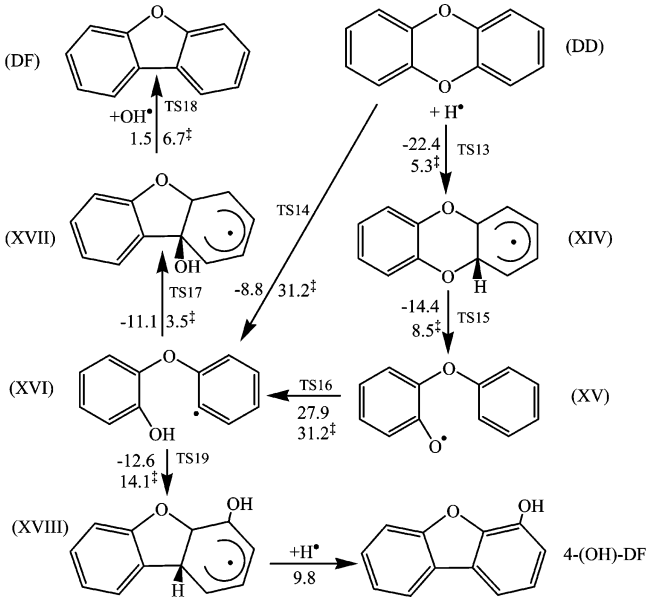


**Figure 6.** Production of DF from the reaction DD + H•. The double dagger symbol after a number denotes an activation energy; no symbol after a number signifies the energy change of a reaction. Both activation and reaction energies were calculated at B3LYP/6-311+G(3df,2p)//B3LYP/6-31G(d) level of theory.

Possible reaction channels between hydrogen atom and DD are shown in Figure 6. In the first channel, a hydrogen atom is ipso-added to the C site of the C−O bridge through TS13. Despite H being distant by 1.836 Å from the C atom, it lengthens the C═C double bond by 0.02 Å. Using the BB1K method, TS13 is located 7.6 kcal/mol above the reactants, while it is 2.3 kcal/mol lower when optimized using B3LYP. Ipso-addition at this site stabilizes the product, 2-phenoxycyclohexa-2,5-dienone (XIV), by 22.4 kcal/mol. The O−C bond in XIV is 0.061 Å longer than the normal C−O bond in DD, leading to facile C−O rupture in a reaction exoergic by 14.4 kcal/mol to form the adduct 2-phenoxycyclohexa-2,5-dienone (XV). Bond breakage of the (H)C−O bond in XIV requires only 8.5 kcal/mol activation energy through the transition structure of TS15. XV lies 36.6 kcal/mol below the reactants DD + H. Although intermolecular H transfer from C to the phenoxy O in XV to

produce 2-phenoxycyclohexa-2,5-dienol (XVI) requires an activation energy (with respect to XV) of 31.2 kcal/mol, the overall reaction energy is still below that of the separated reactants. XVI can also be formed through direct H addition to O via TS14 with a relatively high barrier of 37.5 kcal/mol using the BB1K method, a value which is higher by 5.9 kcal/mol than that calculated by B3LYP. Thus, it is expected that H addition at the C site as opposed to addition to the O site will dominate both energetically and also statistically (four C addition sites versus two O sites).

As explained by Cieplik et al.,[11] XVI is the precursor for the major DD pyrolysis product, DF, and for 4-hydroxydibenzofuran, traces of which were detected experimentally. Ring closure at the ring carbon radical site of XVI and the C atom bearing the hydroxyl group produces the DF hydroxyl derivative XVII through TS17, which is located 3.5 kcal/mol above XVI. C-radical site attack at the carbon neighboring O in the other benzene ring affords XVII, a direct precursor for 4-hydroxydibenzofuran via TS19. This transition state is higher by 10.6 kcal/mol than TS14. The difference in energy barriers highlights why DF is a major DD pyrolysis product whereas 4-hydroxydibenzofuran is not. Hydroxyl group expulsion from XVII via TS18 produces DF. The whole mechanism (DD + H $\rightarrow$ DF + OH) is exoergic by 18.4 kcal/mol (at 0 K).

The barrier height for H addition to the carbon atom bonded to oxygen in OCDD was also calculated by the BB1K method and found to be only 0.3 kcal/mol lower than the barrier height for the analogous reaction with the nonchlorinated congener (DD) where our best value for the barrier height using the BB1K method is 7.6 kcal/mol. On the basis of results from this study and from a previous study,[14] three H reaction channels with OCDD may be compared, viz., H addition to C−O carbon atoms, H addition to carbon bearing a Cl atom followed by Cl elimination, and direct abstraction of Cl by H to form HCl. Caution must be taken in making this comparison, because the range of computational errors in the barrier heights would be at least 2−3 kcal/mol when comparing results from the different computational methods used (BB1K and B3LYP in this study and B3PW91/3-21G** in the case of Fueno et al.[14]). We find that H attack on the C site of the C−O bridge has a comparable barrier to chlorine abstraction to form HCl (7.3 kcal/mol compared with 8.8 kcal/mol[14]), and the statistical factors (four sites in DD for C−O against eight sites for C−Cl/H in prechlorinated DD) determine the competition between Cl expulsion and C−O ring opening where the barriers for the two processes are similar (7.3 kcal/mol compared with 5.3 kcal/mol[14]).

In pyrolysis, one finds up to 400 times more PCDF (mainly lower chlorinated congeners) than PCDD, while in typical incineration, PCDD/F homologue profiles are usually dominated by PCDD.[4] It is clear that the lower chlorinated PCDF congeners result in part from Cl expulsion caused by ipso-addition of the ubiquitous hydrogen radicals in pyrolysis. Ipso-H addition at the four C sites of the four C−O bonds readily converts DD into DF. This no doubt plays a major role in producing a different ratio of PCDD to PCDF in pyrolysis than in typical incineration.

## 4. Conclusions

We have used DFT(B3LYP and BB1K) to determine optimized structures of reactants, products, and transition states involved in the reactions of DF + H, DF + $H_2$, and DD + H in addition to the unimolecular decomposition of DF. According to these calculations, self-decomposition of DF initiated by a $\beta$-bond scission of the C−O bridge would not be significant, owing to its high energy barrier. While the energy requirements of H self-expulsion and C−O bond scission are very similar, entropic effects are expected to favor H self-expulsion as the most accessible corridor for unimolecular decomposition of DF. Bimolecular reaction with a hydrogen molecule is shown to have two energetically feasible channels, ipso-additions of two H atoms at sites 1 and 9 of DF and addition to O and C on the edge of the central bridge C−O. The first of these reactions is more favorable, having an activation barrier of 21.3 kcal/mol less than the latter.

DF was shown to admit four reaction channels with H, viz., addition at C−O carbon, addition at C−O oxygen, addition at the C−C carbon bridge in the five membered ring, and addition to C atoms of the benzene rings. All addition products are more stable than the separated reactants. Direct C−O bond fission through H addition to the C−O oxygen is expected to be slow when compared with other available channels, especially H addition to the C−O carbon followed by rupture of the resultant C(H)−O bond. A detailed mechanism for DD conversion into DF and hydroxyl-DF comprises H addition to the C−O carbon followed by C(H)−O bond fission and H transfer from H to the C−O oxygen, to result in the structure (XVI) which is a direct precursor for DF and hydroxyl-DF. These reactions should be of great importance in waste management applications where the PCDD/F profile is dominated by DF congeners. This hypothesis has been tested for OCDD congener where comparison has been made with literature data for other available channels such as H addition to carbon bearing Cl atoms and direct Cl abstraction to form HCl. H addition to the C−O carbon in OCDD was found to be at least as fast as the other two channels, taking into account the shortcoming of the computational methods in predicting the energy barriers.

**Acknowledgment.** This research has been supported by a grant from the Australian Research Council. M.A. acknowledges the award of a postgraduate studentship by the Al-Hussein Bin Talal University (Jordan).

**Supporting Information Available:** Calculated total energies, zero-point energies, Cartesian coordinates, moments of inertia, and vibrational frequencies of all equilibrium and transition states structures. This material is available free of charge via the Internet at http://pubs.acs.org.

## References and Notes

(1) Van den Berg, M.; De Jongh, J. H, P.; Olson, J. R. *Crit. Rev. Toxicol.* **1994**, *24*, 1.
(2) Bumb, R. R.; Crummett, W. B.; Cutie, S. S.; Gledhill, J. R.; Hummel, R. H.; Kagel, R. O.; Lamparski, L. L.; Luoma, E. V.; Miller, D. L.; Nestrick, T. J.; Shadoff, L. A.; Stehl, R. H.; Woods, J. S. *Science* **1980**, *210*, 385.
(3) Calaminus, B.; Fiedler, H.; Stahlberg, R. *Organohalogen Compd.* **1997**, *31*, 354.
(4) Weber, R.; Sakurai, T. *Chemosphere* **2001**, *45*, 1111.
(5) Rosemann, R.; Lorenz, W.; Bahadir, M.; Hopf, H. *Fres. Environ. Bull.* **1998**, *7*, 289.
(6) Mohr, K.; Nonn, C.; Jager, J. *Chemosphere* **1997**, *34*, 1053.
(7) Yamamoto, T.; Inoue, S.; Sawachi, M. *Chemosphere* **1989**, *19*, 271.
(8) Evans, C. S.; Dellinger, B. *Environ. Sci. Technol.* **2003**, *37*, 1325.
(9) Evans, C. S.; Dellinger, B. *Environ. Sci. Technol.* **2005**, *39*, 122.
(10) Altarawneh, M.; Dlugogorski, B. Z.; Kennedy, E. M.; Mackie, J. C. *J. Phys. Chem. A* **2007**, *111*, 2563.
(11) Cieplik, M. K.; Epama, O. J.; Louw, R. *Eur. J. Org. Chem.* **2002**, *2002*, 2792.
(12) Winkler, J. K.; Karow, W.; Rademacher, P. *J. Anal. Appl. Pyrol.* **2001**, *57*, 133.
(13) Altarawneh, M.; Dlugogorski, B. Z.; Kennedy, E. M.; Mackie, J. C. *J. Phys. Chem. A* **2006**, *110*, 13560.
(14) Fueno, H.; Tanaka, K.; Sugawa, S. *Chemosphere* **2002**, *48*, 771.

(15) Okamoto, Y. *Chem. Phys. Lett.* **1999**, *310*, 355.
(16) Frisch, M. J.; Trucks, G. W.; Schlegel, H. B.; Scuseria, G. E.; Robb, M. A.; Cheeseman, J. R.; Montgomery, J. A., Jr.; Vreven, T.; Kudin, K. N.; Burant, J. C.; Millam, J. M.; Iyengar, S. S.; Tomasi, J.; Barone, V.; Mennucci, B.; Cossi, M.; Scalmani, G.; Rega, N.; Petersson, G. A.; Nakatsuji, H.; Hada, M.; Ehara, M.; Toyota, K.; Fukuda, R.; Hasegawa, J.; Ishida, M.; Nakajima, T.; Honda, Y.; Kitao, O.; Nakai, H.; Klene, M.; Li, X.; Knox, J. E.; Hratchian, H. P.; Cross, J. B.; Bakken, V.; Adamo, C.; Jaramillo, J.; Gomperts, R.; Stratmann, R. E.; Yazyev, O.; Austin, A. J.; Cammi, R.; Pomelli, C.; Ochterski, J. W.; Ayala, P. Y.; Morokuma, K.; Voth, G. A.; Salvador, P.; Dannenberg, J. J.; Zakrzewski, V. G.; Dapprich, S.; Daniels, A. D.; Strain, M. C.; Farkas, O.; Malick, D. K.; Rabuck, A. D.; Raghavachari, K.; Foresman, J. B.; Ortiz, J. V.; Cui, Q.; Baboul, A. G.; Clifford, S.; Cioslowski, J.; Stefanov, B. B.; Liu, G.; Liashenko, A.; Piskorz, P.; Komaromi, I.; Martin, R. L.; Fox, D. J.; Keith, T.; Al-Laham, M. A.; Peng, C. Y.; Nanayakkara, A.; Challacombe, M.; Gill, P. M. W.; Johnson, B.; Chen, W.; Wong, M. W.; Gonzalez, C.; Pople, J. A. *Gaussian 03*, revision A.11; Gaussian, Inc.: Pittsburgh, PA, 2001.
(17) Becke, A. D. *J. Chem. Phys.* **1993**, *98*, 5648.
(18) Lee, C.; Yang, W.; Parr, R. G. *Phys. Rev. B* **1988**, *37*, 785 LP
(19) Montgomery, J. A.; Ochterski, J. W.; Petersson, G. A. *J. Chem. Phys.* **1994**, *101*, 5900.
(20) Zhu, L.; Bozzelli, J. W. *J. Phys. Chem. Ref. Data* **2003**, *32*, 1713.
(21) Pimenova, S. M.; Melkhanova, S. V.; Kolesov, V. P.; Demyanov, P. I.; Fedotov, A. N.; Vorobieva, V. P. *J. Chem. Therm.* **2002**, *34*, 385.
(22) Chirico, R. D.; Gammon, B. E.; Knipmeyer, S. E.; Nguyen, A.; Strube, M. M.; Tsonopoulos, C.; Steele, W. V. *J. Chem. Therm.* **1990**, *22*, 1075.
(23) Okamoto, Y.; Tomonari, M. *J. Phys. Chem. A* **1999**, *103*, 7686.
(24) Polo, V.; Kraka, E.; Cremer, D. *Theor. Chem. Acc.* **2002**, *107*, 291.
(25) Lynch, B. J.; Truhlar, D. G. *J. Phys. Chem. A* **2001**, *105*, 2936.
(26) Durant, J. L. *C. Phys. Lett.* **1996**, *256*, 595.
(27) Zhao, Y.; Lynch, B. J.; Truhlar, D. G. *J. Phys. Chem. A* **2004**, *108*, 2715.
(28) Becke, A. D. *J. Chem. Phys.* **1996**, *104*, 1040.
(29) Zhao, Y.; Gonzalez-Garcia, N.; Truhlar, D. G. *J. Phys. Chem. A* **2005**, *109*, 2012.
(30) Eriksson, L. A.; Kryachko, E. S.; Nguyen, M., T. *Int. J. Quant. Chem.* **2004**, *99*, 841.
(31) Truong, T. N.; Truhlar, D. G. *J. Chem. Phys.* **1990**, *93*, 1761.
(32) Sumathy, R.; Kryachko, E. S. *J. Phys. Chem. A* **2002**, *106*, 510.